Available online at www.sciencedirect.com
ScienceDirect
Cement and Concrete Research 37 (2007) 191 – 199
Cement and Concrete Research

Rheology of fiber-reinforced cementitious materials

Katherine G. Kuder [a,*], Nilufer Ozyurt [b], Edward B. Mu [c,1], Surendra P. Shah [c]

[a] *Department of Civil and Environmental Engineering, Seattle University, 901 12th Ave., Seattle, WA 98122-1090, USA*
[b] *Faculty of Civil Engineering, Istanbul Technical University, Istanbul, 34469, Turkey*
[c] *Center for Advanced Cement-Based Materials/Northwestern University, 2145 Sheridan Rd, Suite A130, Evanston, IL 60208, USA*

Received 17 August 2005; accepted 31 October 2006

Abstract

An improved understanding of the influence of fibers on the rheology of cementitious systems is needed so that fiber reinforcement can be used effectively. However, conventional rheometers are not suitable for testing stiff fiber-reinforced materials. In this study, a parallel plate rheometer that is capable of evaluating the rheology of stiff fiber-reinforced cement paste and mortar systems was designed and built. The governing equations for the rheometer were derived and experimental procedures were developed that yielded reproducible results. A comparative analysis of the custom-built parallel plate rheometer, a commercial rheometer and the values reported in the literature, indicated that the measurements obtained using the rheometer were reasonable. The rheometer was then used to evaluate the rheology of a variety of cement paste systems, including stiff steel fiber-reinforced cement pastes.
© 2006 Elsevier Ltd. All rights reserved.

Keywords: Rheology; Fiber reinforcement

1. Background

Fiber reinforcement is used to improve the brittle nature of cementitious composites. Fibers bridge cracks during loading and transfer the load, arresting the growth and coalescence of cracks. Fiber reinforcement has been shown to improve the ductility, toughness, flexural strength and shear strength of cementitious materials [1,2], to reduce shrinkage cracking and permeability [3,4] and to enhance fatigue and impact resistance [2,5,6]. The efficacy of the fiber reinforcement is dependent upon many factors, including the properties of the matrix as well as the fiber geometry, size, type, volume and dispersion.

Despite the benefits of fiber reinforcement, fibers can make cementitious materials difficult to work with in the fresh state, compromising hardened state properties. Incorporation of fiber reinforcement can make mixing more difficult, resulting in excessive voids as well as difficulties with fiber dispersion. To utilize fiber reinforcement effectively, the fresh state properties of the composite material must be controlled so that it is easy to handle in the fresh state and the hardened state properties are not adversely affected.

2. Introduction

The fresh state characteristics of cementitious materials can be described using rheological parameters. Rheology is the study of material flow, or deformation, under stress. For cementitious materials, rheological parameters help to describe the ease with which it can be used in the fresh state, including workability, placeability, compactability, finishability, flowability, pumpability and extrudability. Different applications require different rheological characteristics. By understanding the rheology of basic cementitious materials, mix designs can be tailored to the desired applications, including advanced systems such as fiber-reinforced concrete.

A number of different models exist to describe the rheological characteristics of cementitious systems. The most commonly used model is the Bingham model, which is given by:

$$\tau = \tau_0 + \mu_0 \dot{\gamma} \tag{1}$$

* Corresponding author. Tel.: +1 206 296 2246; fax: +1 206 296 2173.
E-mail address: kuderk@seattleu.edu (K.G. Kuder).
[1] Present address: James Hardie Research, 10901 Elm Avenue, Fontanta, CA 92337, USA.

0008-8846/$ - see front matter © 2006 Elsevier Ltd. All rights reserved.
doi:10.1016/j.cemconres.2006.10.015

where τ_0 is the Bingham yield stress, describing the stress needed to initiate flow, μ_0 is the Bingham plastic viscosity, which is the resistance of the material to flow, and τ and $\dot{\gamma}$ are the shear stress and shear rate, respectively. Other models include the Herschel-Bulkley, Vom Berg, Casson, Ellis, Erying, Robertson-Stiff, Williamson, Sisko and Atzeni, and are reviewed in Malek and Roy [7].

Fig. 1 shows the typical shear stress versus time behavior for a cementitious material being sheared at a constant rate. Both a peak and equilibrium stress are observed due to the thixotropic nature of the material. Under a constant shear rate, there is a time-dependent decrease in viscosity, which can be explained by the microstructural breakdown of the material. Once the shear stress is removed, the microstructure rebuilds. Rheological measuring protocols are based either on the peak stress value, τ_{peak}, or on the equilibrium stress value, $\tau_{equilibrium}$.

Rheometers are used to measure the rheology of cementitious materials. Two categories of rheometers exist: commercially available and custom-designed and -built. Commercially available rheometers were originally developed to test polymer systems. These rheometers allow for different geometries, such as the parallel plate, coaxial cylinder and vane configurations, to be used with one machine by simply changing fixtures. However, sample sizes must be small and the torque capacity is low, limiting testing to relatively fluid cement paste and mortar systems, typically without fiber reinforcement. In response to these limitations, a number of researchers have developed rheometers for evaluating the rheology of highly fluid concrete materials. Custom-designed and -built rheometers include mixer-type setups like the IBB and Two-Point [8–10], coaxial cylinder configurations, such as the BML and CEMAGREF-IMG [11,12] and parallel plate geometries, including the BTRHEOM [13] as well as the rheometer developed at the University of Illinois at Urbana-Champaign [9].

A considerable amount of research has been conducted on the rheology of cementitious materials using both commercial and custom-designed rheometers. Unfortunately, the results from independent studies are not quantitatively comparable due to differences in materials, shear history (mixing/handling procedures), age (hydration), rheology-measuring protocols and the rheometers used [12,14–17]. In addition, testing artifacts, such as plug flow, wall slip, sedimentation and edge effects, can significantly influence rheological measurements. When reviewing the values reported in the literature, Tattersall and Banfill found a 20-fold and 50-fold range for yield stress and viscosity measurements, respectively [14]. More recently, custom-built concrete rheometers were compared in a survey at LCPC [16]. They found that even with the same materials and mixing procedures, large variations of yield stress and viscosity values existed. It was noted, however, that a qualitative comparison could be made and that there was a good correlation between the rheometers.

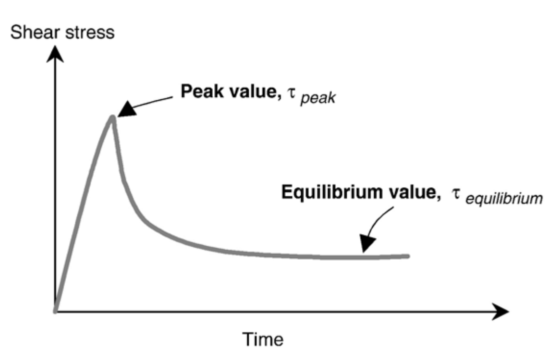

Fig. 1. Peak and equilibrium values of shear stress at a constant shear rate.

In this study, a parallel plate rheometer is designed and built to evaluate the flow behavior of stiff fiber-reinforced systems. Initial experiments are conducted to verify that the rheometer provides reasonable results and to develop appropriate experimental procedures. The effects of water/cement ratio and sand addition on the flow behavior of cement paste systems are then determined. Finally, the influence of steel fibers on the rheology of stiff fiber-reinforced systems is evaluated.

3. Rheometer design

The intent of this work was to design a rheometer that can evaluate the rheological behavior of stiff fiber-reinforced cement paste and mortar systems. With this in mind, a number of considerations were made while selecting the rheometer configuration. First, an adequate gap size was required so that fibers and sand particles could be included in the mix. Next, the occurrence of plug flow and wall slip, testing artifacts which can lead to underestimated rheological parameters, needed to be minimized. Finally, for the rheometer to be able to shear stiff materials, a high-torque capacity motor was needed.

Based on these design considerations, a parallel plate setup (shown in Fig. 2) was selected [18]. The two plates are 254 mm in diameter, with an adjustable gap. The rheometer is equipped with a high torque capacity motor, capable of approximately 20 N m. The upper plate is rotated at a controlled speed. The shear rate varies along the radius of the plates, reducing the occurrence of plug flow. Square grooves, measuring $6.3 \times 6.3 \times 2.5$ mm^3, are machined onto the two plates to minimize slip. A plexi-glass wall surrounds the bottom stationary plate to prevent material from flowing away during testing, which will introduce a frictional effect that will influence the rheological measurements. To reduce the effect of the wall, a large diameter to gap ratio was used (typically greater than 10). The rheometer is attached to a data acquisition system for continuous monitoring during testing.

3.1. Governing equations

Without a wall, the shear rate, $\dot{\gamma}$ (s^{-1}), between the two plates, is a function of the radius, r (m), and gap height, h (m):

$$\dot{\gamma} = \frac{r\omega}{h} \tag{2}$$

where ω is the rotation rate at the top of the plate (rad/s). For this rheometer, the gap height is assumed to be the clear distance between the grooves. The viscosity of the material can be explicitly expressed as [19]:

$$\eta(\dot{\gamma}_R) = \frac{(T/2\pi R^3)}{\gamma_R}\left[3 + \frac{\mathrm{dln}(T/2\pi R^3)}{\mathrm{dln}\gamma_R}\right] \tag{3}$$

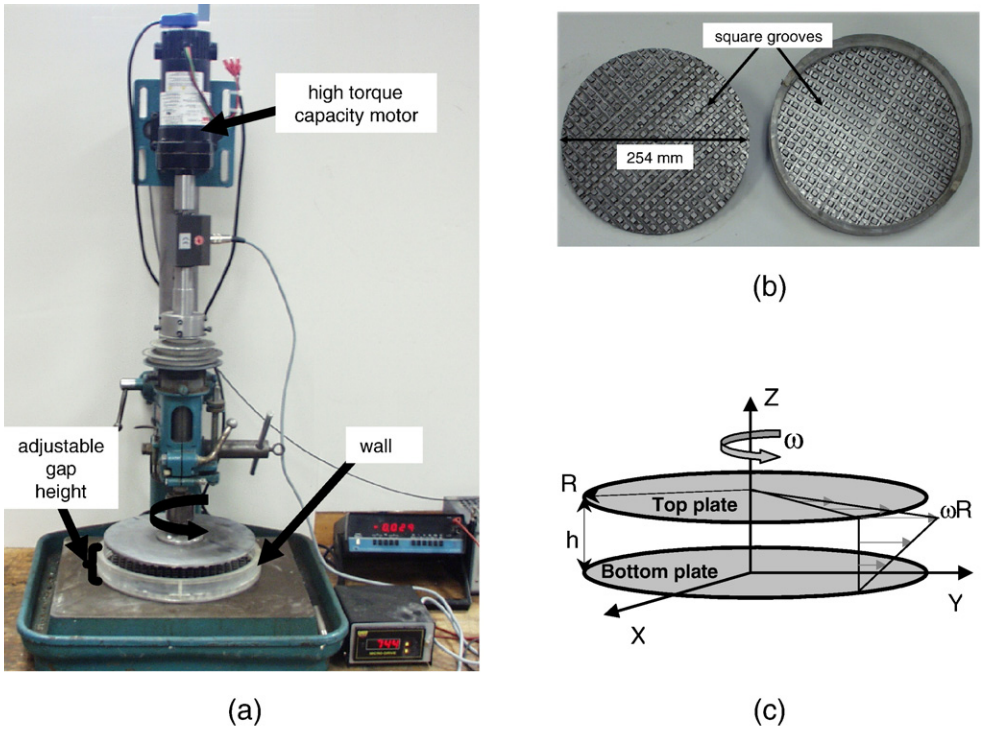

Fig. 2. Parallel plate rheometer built: (a) rheometer, (b) plates with square grooves and (c) velocity distributions.

where $\eta(\dot{\gamma}_R)$ is the shear rate-dependent viscosity (Pa* s), T is the resistant torque (N* m) and $\dot{\gamma}_R$ is the apparent shear rate (shear rate at $r=R$, with R=radius of plate (m)). For a Bingham material, this relationship can be described as a function of rheometer geometry, rotation speed and torque:

$$\frac{T}{\frac{2}{3}\pi R^3} = \tau_0 + \left(\frac{3}{4}\frac{R}{h}\omega\right)\mu_0 \tag{4}$$

where τ_0 is the Bingham yield stress (Pa) and μ_0 is the Bingham viscosity (Pa* s).

If a cylindrical wall is attached to the stationary bottom plate, it will remain static during the test. From a microscopic viewpoint, there will be an interfacial layer between the wall and the measured material. Various authors have proposed the following model to describe this phenomenon [20]:

$$\tau = \tau_{0,\mathrm{i}} + \eta_0 v_{\mathrm{g}} \tag{5}$$

where τ is the shear stress (Pa), $\tau_{0,\mathrm{i}}$ is the interfacial yield stress (Pa), η_0 is the interfacial viscous constant (Pa* s/m) and v_{g} is the sliding velocity (m/s). Then, the total torque required should be a summation of the resistant torque by the measured material, which is the same as Eq. (2), and the resistant torque by the cylindrical wall (v_{g} is assumed to be linearly distributed along the gap):

$$\frac{T}{\frac{2}{3}\pi R^3} = \left(\tau_0 + \frac{3h}{R}\tau_{0,\mathrm{i}}\right) + \left(\frac{3}{4}\frac{R}{h}\omega\right)\left(\mu_0 + \frac{2\eta_0 h^2}{R}\right) \tag{6}$$

From the torque–rotation relationship, the Bingham parameters, τ_0 and μ_0, can be obtained, if the boundary conditions of the wall are known. Eq. (6) suggests that the wall effect is more significant as the gap height increases.

3.2. Experimental determination of wall effect

To understand the influence of the wall on the rheological measurements, the flow behavior of a standardized known-viscosity oil (Cannon N15000 viscosity standard: 66 Pa* s at 20 °C) was evaluated. Using Eq. (3), the viscosity was measured at a variety of gap heights. The lowest gap height corresponded to a clear distance between the grooves that was equal to twice the total groove height (10 mm), since the teeth effect will become more pronounced at lower gap heights.

Fig. 3 presents the measured viscosity as a function of gap height. As the model predicts, the viscosity increases with increasing gap height, due to the wall effect. Based on Eq. (6), a

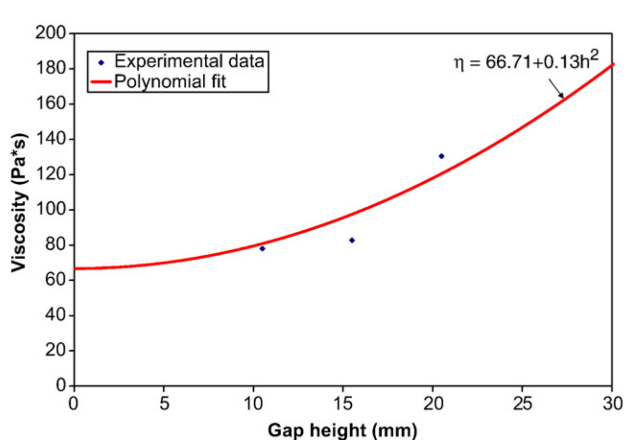

Fig. 3. Viscosity as a function of gap height for known-viscosity oil.

second-order polynomial curve is fit to the data. By obtaining the viscosity at a gap height of 0 mm, the wall effect is theoretically eliminated. Experimentally, the value of the polynomial curve at a gap height of 0 mm, minimizes the effect of the wall. Here, the polynomial curve fits the data well and predicts a viscosity of 66.7 Pa* s, with an error of approximately 1%. To minimize the total number of experiments, an optimal range was selected in which the wall effect (more pronounced at larger gap heights) and teeth effect (more pronounced at lower gap heights) should be minimized. This range was estimated to be between 10 and 13 mm.

3.3. Rheological protocol

The rheological measuring protocol used to obtain the equilibrium shear stress values is shown in Fig. 4. This protocol is similar to the one proposed by Geiker et al. [21]. At each shear rate, torque measurements were recorded for 20 s. The torque at each shear rate was then obtained by averaging the values that corresponded to the equilibrium region. To ensure that a steady-state condition was reached, the data from the highest rotation rate was neglected. Torque and rotation speed were converted to shear stress and shear rate. As Fig. 5 demonstrates, shear stress was plotted as a function of shear rate to obtain the Bingham parameters (Eq. (1)). The yield stress was determined from the resultant shear stress versus shear rate data for the slowest two shear rates, since the yield stress corresponds to the shear stress at a shear rate of 0 mm.

3.4. Comparison of parallel plate rheometer, a commercial rheometer and values in literature

To verify that the rheological measurements obtained with the parallel plate rheometer were reasonable, measurements were compared with values determined using a commercial rheometer as well as with findings reported in the literature.

The same materials and mixing procedure were used for both the parallel plate and the Haake rheometer. Samples were mixed in a Hobart (planetary) mixer. Lafarge Type I Portland cement was used. The mixing procedure was as follows: First, the cement was placed in the mixing bowl. Water was added, followed by a 30-s rest. Next, the material was mixed for 30 s on

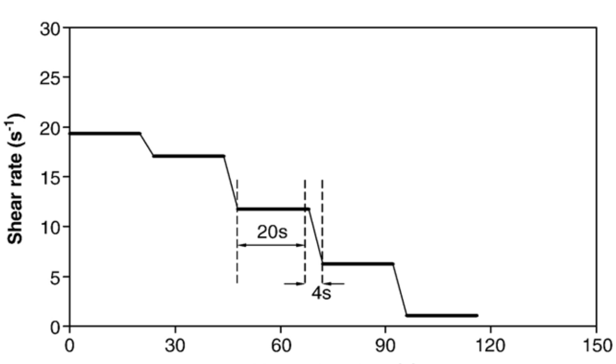

Fig. 4. Rheology measuring protocol.

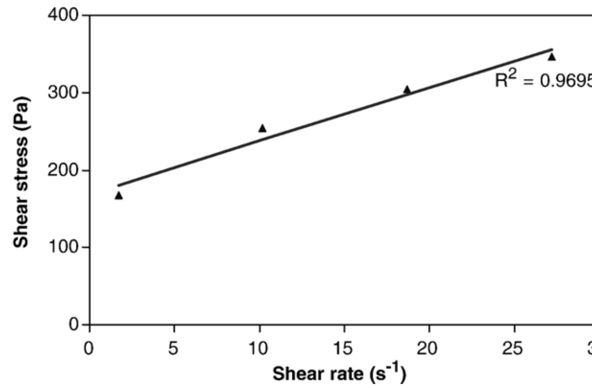

Fig. 5. Example of shear stress vs. shear rate behavior using Bingham fit to data.

the lowest speed. Then, the mixer was stopped and there was a 30-s rest, during which the bowl was scraped to collect any undistributed material. Finally, the material was mixed for 1 min at medium speed.

Neat cement pastes, with water/cement ratios (w/c) = 0.30 and 0.35, were tested with both rheometers. Initially, the parallel plate rheometer measurements were to be compared to the results from a commercial rheometer, a Haake Rheostress 150, using the concentric cylinder configuration. The results, however, were not comparable, with the parallel plate rheometer providing yield stress and viscosity values that were significantly higher than those obtained using the Haake rheometer. It is suspected that this discrepancy is due to the problems of plug flow and slip that are often encountered when using the concentric cylinder geometry [15,22]. Therefore, the fixturing was changed to the vane configuration, which previous researchers have shown to eliminate slip and plug flow [19,23,24]. Saak et al. compared yield stress values obtained using the concentric cylinder geometry and the vane viscometer [15]. For identical cement pastes, a 50% increase in yield stress values was observed due to the elimination of slip and plug flow. With the vane viscometer, only a thin layer of unknown thickness is sheared. Consequently, only rotation rates are known, not shear rates. For this reason, the vane was used to measure yield stress, not viscosity. Both peak and equilibrium yield stress values were obtained using the methodology presented by Saak and colleagues [15].

The parallel plate rheometer was designed to obtain equilibrium shear stress values, using the protocol shown in Fig. 4. To determine the peak equilibrium stress, the shear stress vs. time behavior was only observed for a single shear rate, approximately 1 s^{-1}. This value is not considered to be the absolute value for the peak yield stress, but is rather shown only to identify the range of yield stress values that could be expected from the parallel plate rheometer for a given material, so that comparisons with the vane configuration can be made.

A comparison of the yield stresses measured with the parallel plate rheometer, the vane and by the other researchers for neat paste with water/cement = 0.30 and 0.35 is presented in Figs. 6 and 7, respectively. Yield stress values from other researchers represent the range reported in literature, demonstrating the

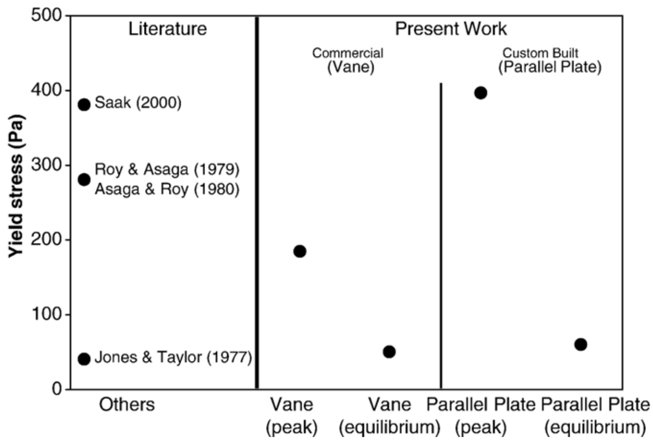

Fig. 6. Comparison of yield stress values for w/c = 0.30.

influence of varying materials, rheometer geometries and measuring procedures on rheological findings. Despite the large range seen, the results obtained by the parallel plate rheometer are comparable.

4. Rheological measurements with the parallel plate rheometer

The parallel plate rheometer was used to study a variety of cementitious systems. To begin, a testing procedure that yielded consistent results with reasonable experimental variation was developed with the neat paste. Then, the influence of w/c and sand on the rheology of cementitious systems was investigated. Finally, the effect of the volume of steel fibers on the rheology of cement paste was studied.

4.1. Repeatability

To investigate the repeatability of the measurements made with the parallel plate rheometer, the rheology of two neat cement pastes were examined, with w/c = 0.30 and 0.35. The mixing and measuring protocol described previously in Sections 3.4 and 3.3, respectively, were used. After mixing, the fresh cement paste was put into the rheometer with a scraper and then leveled by hand. Three repetitions were made.

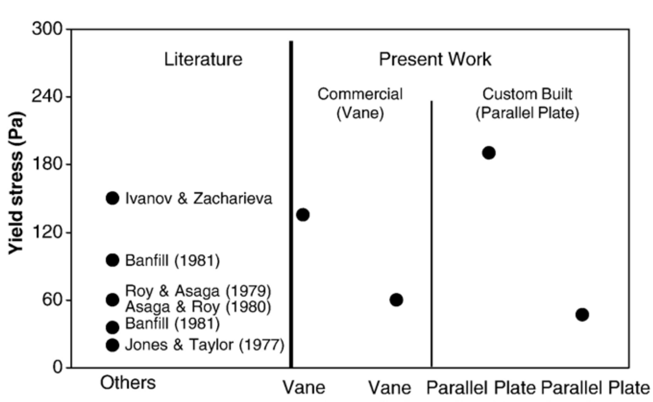

Fig. 7. Comparison between yield stress values for w/c = 0.35.

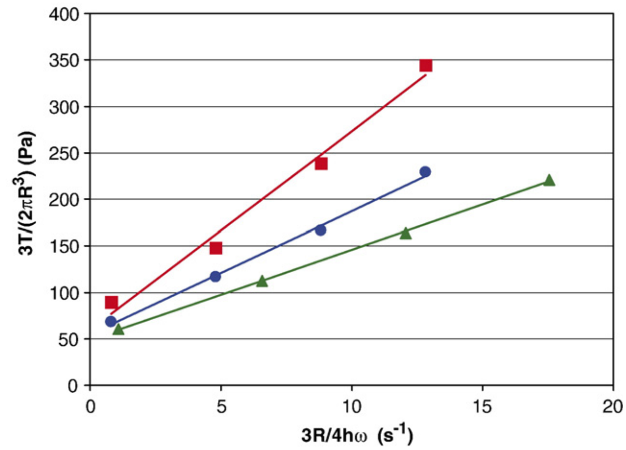

Fig. 8. Rheological measurements for cement paste with w/c = 0.30 with no vibration.

Fig. 8 presents experimental results using the procedure described. The three replications are shown separately and they demonstrate that utilization of this preparation technique resulted in large experimental variations. Due to the stiffness of the matrices, the surface of the fresh cement paste was uneven, making it difficult to ensure that the top rheometer plate came in complete contact with the material. In addition, differences in void contents from sample to sample could have been large.

To reduce measurement variations, the testing procedure was modified. After the fresh sample was placed into the rheometer, a normal compression force of 2.36 kg was applied on the top of the sample as it was vibrated for 10 s. A FMC Technologies vibration table, model VP-51-D1, which operates at 3600 V/min on 60 Hz of power was used. Vibration was applied at the highest setting with a stroke of approximately 0.015 in. Results from applying the vibration are shown in Fig. 9, demonstrating an improvement in repeatability. This procedure was found to make the surface more level and it is suspected that it also made the void system more uniform. Similar results were found with the w/c = 0.35.

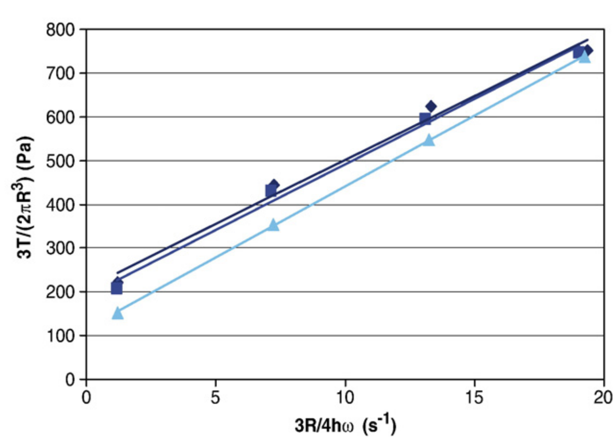

Fig. 9. Rheological measurements for cement paste with w/c = 0.30 with normal compression and vibration.

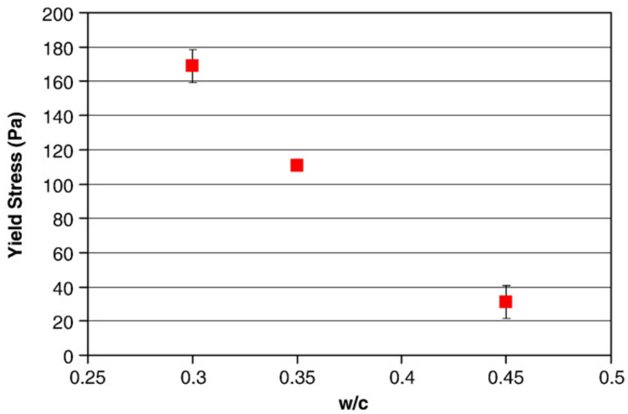

Fig. 10. Effect of w/c on yield stress of cement paste (with standard deviations).

4.2. Experimental procedures

Subsequent rheological testing employed the vibratory preparation technique described above. In addition, a more rigorous mixing procedure was used: First, the cement, sand and fibers (if applicable) were placed in a Hobart mixer and mixed for 1 min at low speed. Next, water was added and the material mixed for 1 min at low speed and then there was a 30-s rest. Finally, the materials were mixed for 2 min at high speed. This procedure was selected because it was found to disperse the sand and fibers well. The rheological measuring protocol given in Fig. 4 was used. The gap height between the plates was kept between 10 and 13 mm. At least three replications were made for each parameter investigated.

The cement was Lafarge Type I. Short steel fibers, produced by Bekaert, which had a length of 6 mm and a diameter of 0.16 mm, were used. River sand, with a maximum particle diameter of 3 mm, was used in the oven-dry condition.

4.3. Results

4.3.1. Cement paste

The influence of w/c on the rheological parameters for neat paste was evaluated. Three different neat pastes were studied, with w/c = 0.30, 0.35 and 0.45. As is expected, and Figs. 10 and 11 demonstrates, both the yield stress and viscosity, respectively, decrease as the w/c increases.

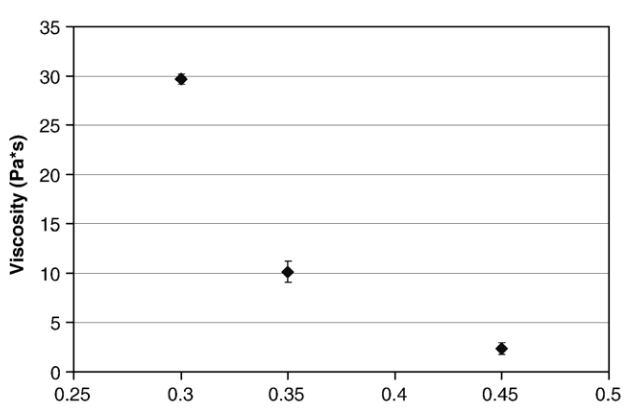

Fig. 11. Effect of w/c on viscosity of cement paste (with standard deviations).

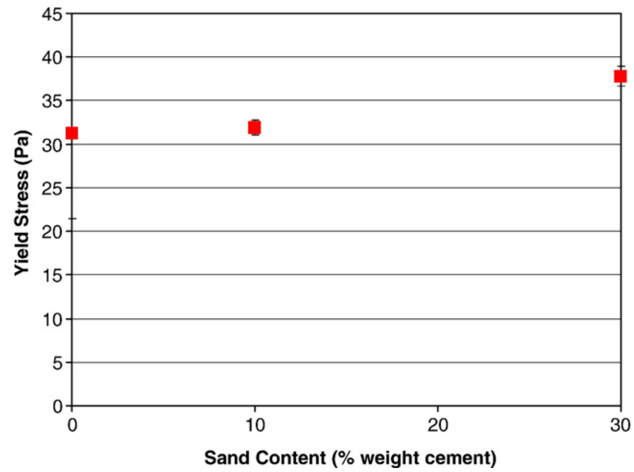

Fig. 12. Effect of sand content on yield stress of cement paste with w/c = 0.45 (with standard deviations).

Figs. 12 and 13 present the effect of sand addition on the rheology of cement paste with a w/c = 0.45. Sand was added at 10% and 30% of the cement mass. Addition of sand has a small influence on the yield stress, but has a significant effect on the viscosity, which increases by more than four times, from 0% to 30% sand.

4.3.2. Fiber-reinforced cement pastes

Finally, the rheology of steel fiber-reinforced cement paste was determined. Two w/c, 0.30 and 0.35, with three fiber volume contents, 1%, 2% and 4%, were studied. Figs. 14 and 15 show the effect of steel fiber volume on the yield stress and viscosity of the neat pastes, respectively. For both w/c, the yield stress decreases until a critical volume fraction is reached, and then increases. The viscosities appear to decrease until reaching a critical point, however, the decrease for the stiffer matrix, with

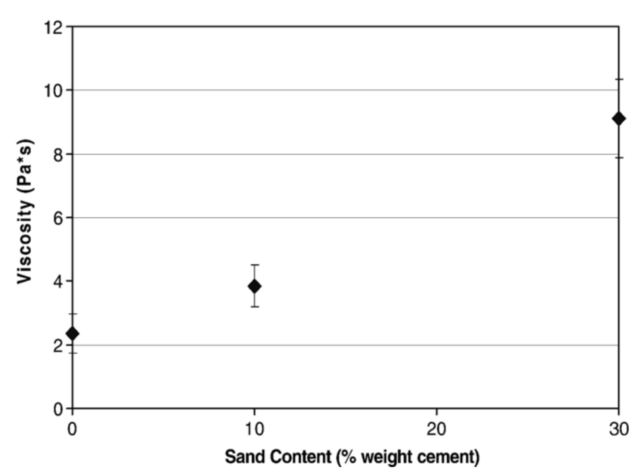

Fig. 13. Effect of sand content on viscosity of cement paste with w/c = 0.45 (with standard deviations).

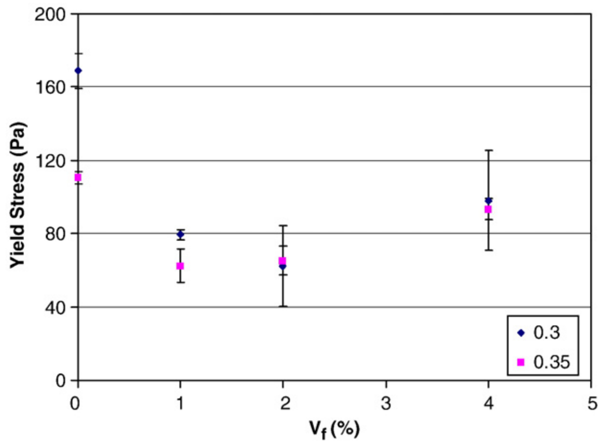

Fig. 14. Effect of fiber content on yield stress of cement paste for w/c = 0.30 and 0.35 (with standard deviations).

w/c = 0.30, is much greater. At a fiber dosage of 4%, the yield stress and viscosity are similar for both w/c.

5. Comparative analysis

Generally, it is expected that adding fibers will increase the yield stress and viscosity of cementitious materials. However, little research has been done on the rheology of fiber-reinforced cementitious materials, and most of the work has been done on highly fluid concrete or mortar, not on stiff cement paste systems. To evaluate the influence of steel fibers on the rheology of a more fluid material, and to compare rheological measurements from the parallel plate rheometer to those obtained using another custom-designed and built rheometer, the rheology of a highly fluid steel fiber-reinforced mortar was studied. In addition, drop table experiments were conducted.

5.1. Rheology of highly fluid steel fiber-reinforced mortar

Previous researchers evaluated the rheology of a highly fluid steel fiber-reinforced mortar using the BML rheometer

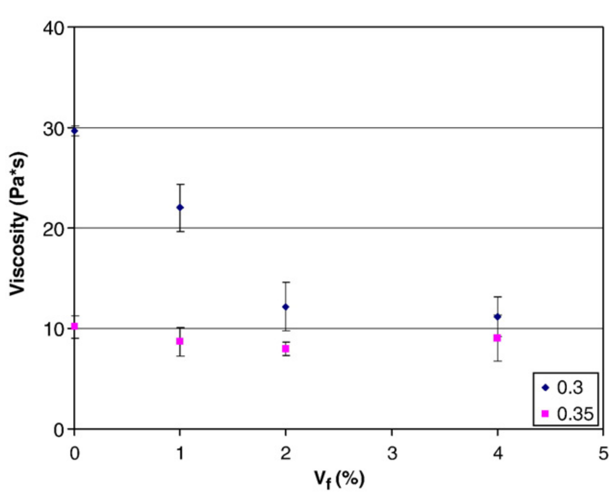

Fig. 15. Effect of fiber content on viscosity of cement paste for w/c = 0.30 and 0.35 (with standard deviations).

Table 1
Comparison of parallel plate and BML rheometer [25]

V_f (%)	Parallel plate		Bui and colleagues	
	Yield stress (Pa)	Viscosity (Pa*s)	Yield stress (Pa)	Viscosity (Pa*s)
0	25.6	4.51	16	1
1	27.1	4.82	27	2
2	51.4	5.74	34	3.4

(concentric cylinder) that was developed by Wallevik and Gjorv [12,25]. In their work, Bui and colleagues [25] used steel fibers that are similar to the fibers in this study and found that as the amount of fibers increased, the Bingham yield stress and viscosity increased. These experiments were repeated in this study. The mixture proportions are as follows: cement = 592 kg/m^3, water = 355 kg/m^3, sand = 1184 kg/m^3 (water/cement = 0.6) [25]. The mixing sequence reported was used; however, the constituent materials varied slightly and the rheological protocol and rheometer were different. Table 1 presents the results of this investigation. The trends observed by the authors are the same as those reported by Bui et al. The absolute values of the rheological parameters are of the same magnitude, but do not match exactly. This discrepancy is expected when using different rheometers and rheology protocols, as discussed previously [14,16]. This work also demonstrates the potential differences in rheological trends when more fluid materials are investigated.

5.2. Drop table

Finally, drop table experiments were preformed. A modified version of ASTM C-109, Standard Test Method for Compressive Strength of Hydraulic Cement Mortars, was used [26]. A frustum mold that is 50 mm in height with a lower diameter of 100 mm and an upper diameter of 70 mm was placed on the drop table apparatus. The material was mixed according the procedure discussed previously (Section 4.2), placed in the mold and vibrated for 10 s. The mold was then removed and the crank turned manually 25 times, each time vertically displacing the table by 12.7 mm. The diameter of the spread material was then measured in four places. These four values were then averaged to give the flow diameter. Three replications were made for each mix tested.

Table 2 presents the drop table results from this test for the fiber-reinforced cement pastes. Similar to the results obtained

Table 2
Drop table results for steel fiber-reinforced cement pastes

w/c	V_f (%)	Flow diameter (mm)
0.3	0	12.69 ± 0.4
	1	12.93 ± 0.7
	2	12.9 ± 0.4
	4	12.54 ± 0.6
0.35	0	14.05 ± 0.4
	1	14.81 ± 0.7
	2	13.82 ± 0.2
	4	15.20 ± 1.0

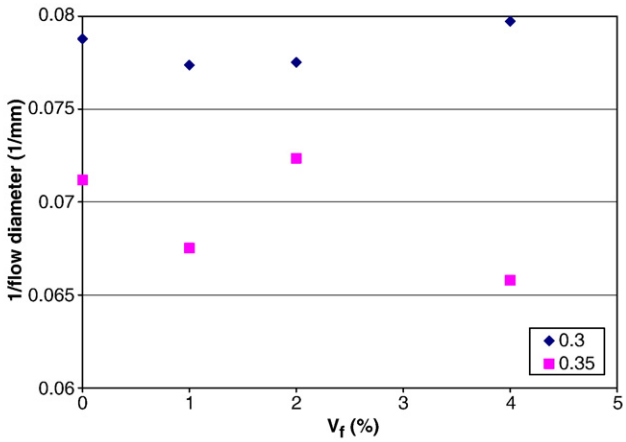

Fig. 16. Effect of fibers on flow diameter.

with the parallel plate rheometer, fibers do not appear to adversely affect the flow behavior of the cement pastes systems, with the flow diameter not significantly changed due to the fibers. Fig. 16 presents the inverse of the flow diameter (an indication of yield stress) as a function of the volume fraction of fiber reinforcement for the cement pastes with w/c=0.30 and 0.35. Generally, the trends observed are similar to those found with the parallel plate rheometer, with the inverse of the flow diameter decreasing as the volume fraction increases until a critical point is reached. However, for the w/c=0.35, with 4% addition of fibers, a decrease is seen, which is not expected. Nevertheless, these results do suggest that there is an initial decrease in the yield stress of the material, followed by an increase once a critical volume fraction of fiber reinforcement is reached.

6. Discussion

The results presented here for the steel fiber-reinforced cement pastes are not what are generally expected. It is hypothesized that the initial decrease in Bingham parameters is due to the thixotropic nature of the cement paste. The stiff steel fibers might increase the amount structural breakdown that occurs during mixing, thus initially reducing the yield stress and viscosity of the material. However, once a certain critical volume fraction of fibers is reached, the mechanical interlocking, or entangling, of the fibers could be dominating the flow behavior. This phenomenon of mechanical fiber interactions has been observed with fiber-reinforced polymers [27]. Thus, at lower fiber dosages, the properties of the cementitious matrices are dominant, which is why the yield stress and viscosity are lower for w/c=0.35 than for w/c=0.30. After the critical volume fraction, the absolute values of the Bingham parameters are much closer, regardless of w/c, suggesting that the fiber interlocking is governing the behavior. It is also interesting to note that the critical volume fraction appears to be higher for the w/c=0.30 than the w/c=0.35, possibly indicating that a stiffer material undergoes more structural breakdown before reaching the critical point.

To isolate the effect of the mechanical interaction of the fibers, the rheology of a Newtonian fluid was evaluated. Rheological measurements were determined for a commercially available honey (Sue Bee Clover Honey) with varying dosages of the steel fibers investigated previously. The results from these experiments are shown in Fig. 17. From 0% to 2%, the change in viscosity is small; however, between 2% and 4%, a large increase in the viscosity is observed. Thus, there does appear to be a point at which the mechanical interlocking of fibers dominates the flow behavior for both Bingham and Newtonian liquids.

7. Conclusion

A parallel plate rheometer was designed and built to evaluate the rheology of stiff fiber-reinforced cement pastes. Initial studies were conducted to verify that the rheometer worked properly. Finally, the rheology of a variety of cement paste systems was studied, including stiff steel fiber-reinforced cement pastes. From this study, the following conclusions can be drawn:

- The parallel plate rheometer yields reasonable rheological parameters. Measurements using the parallel plate rheometer fall within a reasonable range, when compared with the values obtained from a commercial rheometer and those values reported in the literature.
- The frictional effect of the rheometer wall can be modeled using constitutive relations for the interfacial layer that forms between the wall and the bulk material. According to the resultant model, yield stress and viscosity measurements increase as the gap height increases.
- With stiff cementitious materials, high variations in yield stress and viscosity measurements are seen when vibration is not applied, most likely due to the uneven surfaces of the samples and the differing void contents. Repeatability can be improved by applying vibration with normal compression to the sample before testing.
- For the steel fibers investigated, the Bingham rheological parameters decrease until a critical volume fraction is reached. This trend is explained by a coupling effect between the structural breakdown of the material, which occurs at low fiber volumes, and the mechanical interlocking of fiber, which occurs at higher volume fractions.

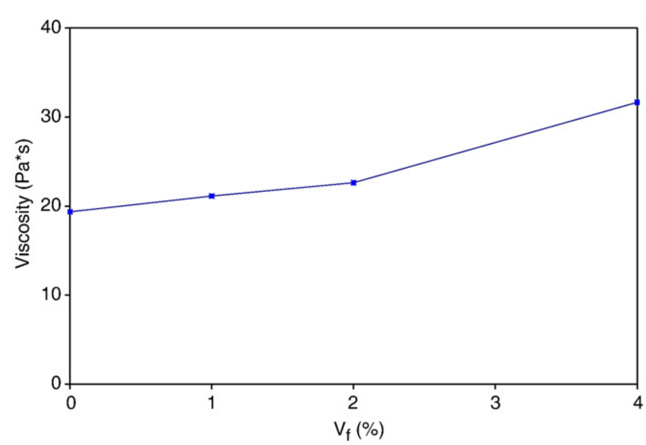

Fig. 17. Effect of fiber content on viscosity of honey.

Acknowledgements

The authors gratefully acknowledge the financial support of Lafarge and WR-Grace. This work was also funded by NSF PATH Grant no. CMS-0122045. The second author would also like to acknowledge the financial support of TUBITAK (The Scientific and Technical Research Council of Turkey) and ITU (Istanbul Technical University). Fibers were provided by Bekaert.

References

[1] E.G. Nawy, Fundamentals of High-Performance Concrete, 2nd ed., John Wiley & Sons, Inc., 2001, p. 464.

[2] P.N. Balaguru, S.P. Shah, Fiber-Reinforced Cement Composites, McGraw-Hill Inc., New York, 1992.

[3] J.S. Lawler, D. Zampini, S.P. Shah, Permeability of cracked hybrid fiber-reinforced mortar under load, ACI Materials Journal 99 (4) (2002) 379–385.

[4] T. Voigt, K.B. Bui, S.P. Shah, Drying shrinkage of concrete reinforced with fibers and welded-wire fabric, ACI Materials Journal 101 (2) (2004) 233–241.

[5] W. Suaris, S.P. Shah, Properties of concrete subjected to impact, Journal of Structural Engineering 109 (7) (1983) 1727–1741.

[6] N. Banthia, S. Mindess, J. Trottier, Impact resistance of steel fiber reinforced concrete, ACI Materials Journal 93 (9) (1996) 472–479.

[7] R.I.A. Malek, D.M. Roy, Modeling the rheological behavior of cement pastes: a review, Advances in Cementitious Materials Ceramic Transactions, The American Ceramic Society, Westerville, OH, 1991, pp. 31–40.

[8] D. Beaupre, Rheology of high performance shotcrete, Civil Engineering, University of British Columbia, British Columbia, 1994.

[9] L.J. Struble, U. Puri, X. Ji, Concrete rheometer, Advances in Cement Research 13 (2) (2001) 53–63.

[10] G.H. Tattersall, S.J. Bloomer, Further development of the two-point test for workability and extension of its range, Magazine of Concrete Research 31 (1979) 202–210.

[11] P. Coussot, Rheologie des Boues et Laves Torrentielles – Etudes de Dispersions et Suspensions Concentrees, L'Institut National Polytechnique de Grenoble, et Etudes du Cemagref, 1993, p. 418.

[12] O.H. Wallevik, O.E. Gjorv, Development of coaxial cylinder viscometer for fresh concrete, Properties of Concrete, RILEM Colloquium, Chapman and Hall, Hanover, 1990, pp. 213–224.

[13] C. Hu, F. de Lallard, T. Sedran, C. Boulay, F. Bosc, F. Deflorenne, Validation of BTRHEOM, the new rheometer for soft-to-fluid concrete, Materials and Structures 29 (1996) 620–631.

[14] G.H. Tattersall, P.F.G. Banfill, The Rheology of Fresh Concrete, Pittman, London, 1983.

[15] A.W. Saak, H.M. Jennings, S.P. Shah, The influence of wall slip on yield stress and viscoelastic measurements of cement paste, Cement and Concrete Research 31 (2001) 205–212.

[16] P.F.G. Banfill, D. Beaupre, F. Chapdelaine, F. de Larrad, P. Domone, L. Nachbaur, T. Sedran, O.H. Wallevik, J. Wallevik, in: C.F. Ferraris, L.E. Brower (Eds.), Comparison of Concrete Rheometers: International Tests at LCPC (Nantes, France) in October 2000, NISTIR 6819, September, 157.

[17] C.F. Ferraris, L.E. Brower, D. Beaupre, F. Chapdelaine, P. Domone, E. Koehler, L. Shen, M. Sonebi, L. Struble, D. Tepke, O. Wallevik, J. Wallevik, in: C.F. Ferraris, L.E. Brower (Eds.), Comparison of Concrete Rheometers: International Tests at MB (Cleveland, OH) in May 2003, 2004.

[18] K.G. Kuder, N. Ozyurt, B. Mu, S.P. Shah, The rheology of fiber-reinforced cement paste evaluated by a parallel plate rheometer, Advances in Concrete through Science and Engineering, International Union of Laboratories and Experts in Construction Materials (RILEM), Northwestern University, Evanston, IL, USA, 2004.

[19] R.B. Bird, R.C. Armstrong, O. Hassager, Dynamics of Polymeric Liquids, vol. 1, John Wiley and Sons, New York, 1987.

[20] R. Browne, P. Bamforth, Tests to establish concrete pumpability, ACI Materials Journal 74 (7) (1977) 4–19.

[21] M.R. Geiker, M. Brandl, L.N. Thrane, D.H. Bager, J. Wallevik, The effect of measuring procedure on the apparent rheological properties of self-compacting concrete, Cement and Concrete Research 32 (2002) 1791–1795.

[22] P.F.G. Banfill, The rheology of fresh cement and concrete – a review, in: G. Grieves, G. Owens (Eds.), 11th International Cement Chemistry Congress, Durban, South Africa, 2003, pp. 50–62.

[23] A. Yahia, K.H. Khayat, Applicability of rheological models to high-performance grouts containing supplementary cementitious materials and viscosity enhancing admixture, Materials and Structures 36 (2003) 402–412.

[24] R. Lapasin, A. Papo, S. Rajgelj, Flow behavior of fresh cement pastes: a comparison of different rheological instruments and techniques, Cement and Concrete Research 13 (1983) 349–356.

[25] V.K. Bui, M.R. Geiker, S.P. Shah, Rheology of fiber-reinforced cementitious materials, High Performance Fiber-Reinforced Cement Composites (HPFRCC4), Springer, Netherlands, 2003, pp. 221–231.

[26] ASTM C109-99, Standard Test Method for Compressive Strength of Hydraulic Cement Mortars (Using 20 in. or 50 mm Cube Specimens), Annual Book of ASTM Standards (2000).

[27] P.R. Sundararajakumar, D.L. Koch, Structure and properties of sheared fiber suspensions with mechanical contacts, Journal of Non-Newtonian Fluid Mechanics 73 (1997) 205–239.